Frontiers in Bioscience Landmark

Front. Biosci. (Landmark Ed) **2025**; 30(5): 26614
https://doi.org/10.31083/FBL26614

Original Research

FCGR1A Alleviates Ischemic Stroke-induced Injury by Promoting Anti-Inflammatory Microglial Polarization via the AMPK–mTOR Signaling Pathway

Meng Liu[1,†], Xuhui Fan[1,†], Dongya Chen[2], Huibin Yao[1], Zhihui Huang[1], Heng Li[1], Qing Zhang[3], Yuqi Wang[1], Haihan Song[4], Yufeng Yan[1,*]

[1]Department of Neurosurgery, Jinshan Hospital, Fudan University, 201508 Shanghai, China
[2]Department of Neurology, Jiangsu University, 212013 Zhenjiang, Jiangsu, China
[3]Shanghai Cyan Medical Co., Ltd, 201200 Shanghai, China
[4]Department of Immunology, DICAT National Biomedical Computation Centre, Vancouver, BC V6B 5A6, Canada
*Correspondence: yanyufeng@fudan.edu.cn (Yufeng Yan)
[†]These authors contributed equally.

Academic Editor: Lin-Hua Jiang
Submitted: 18 September 2024 Revised: 17 February 2025 Accepted: 14 March 2025 Published: 29 April 2025

Abstract

Background: Ischemic stroke triggers inflammatory responses that lead to neuronal damage, with microglial polarization significantly influencing post-stroke inflammation. This study explores the role of Fc gamma receptor Ia (*FCGR1A*) in microglial polarization and its regulatory mechanisms in ischemic stroke. **Methods**: Differentially expressed genes (DEGs) associated with ischemic stroke were identified using the GSE58294 dataset. Hub genes were found by analyzing protein–protein interaction (PPI) networks. BV2 microglia were subjected to oxygen–glucose deprivation/reoxygenation (OGD/R) to mimic ischemic conditions *in vitro*, and *FCGR1A* and inflammatory marker levels were assessed. Besides, BV2 cells were stimulated with lipopolysaccharide (LPS) and interferon-gamma (IFN-γ) to induce M1 polarization, and the effects of *FCGR1A* overexpression and knockdown on cytokine production and microglial polarization were evaluated. The function of the AMP-activated protein kinase (AMPK)-mTOR pathway in regulating microglial polarization was further investigated using the mTOR inhibitor rapamycin (RAP). **Results**: From the 327 DEGs identified, *FCGR1A* was chosen as a hub gene. OGD/R treatment of BV2 cells produced a time-dependent rise in FCGR1A, induction of brown adipocytes 1 (Iba1), and interleukin 6 (IL-6) expression, indicating enhanced inflammation. *FCGR1A* overexpression induced a proinflammatory response and promoted M1 polarization, whereas *FCGR1A* knockdown reduced inflammation and shifted toward an anti-inflammatory M2 phenotype. Inhibition of the mTOR pathway using RAP, combined with *FCGR1A* knockdown, significantly enhanced AMPK activation and promoted a shift toward an anti-inflammatory M2 phenotype. **Conclusion**: *FCGR1A* modulates microglial polarization by affecting the AMPK–mTOR signaling pathway in ischemic conditions. Targeting *FCGR1A* and related pathways could offer new therapeutic strategies to lessen inflammation and facilitate the healing process after an ischemic stroke.

Keywords: ischemic stroke; *FCGR1A*; AMPK–mTOR signaling pathway; microglial polarization; inflammation

1. Introduction

Stroke, a severe neurological condition, is defined by the abrupt stoppage of blood flow to a particular brain area, resulting in a significant loss of neurologic function [1]. Ischemic stroke, the most prevalent form, is driven by several risk factors, such as atrial fibrillation, smoking, diabetes, hypertension, and hyperlipidemia [2]. Despite advances in preventive measures, stroke remains a major global contributor to morbidity and mortality [3]. The high incidence rates and substantial long-term disability in survivors highlight the ongoing challenge of ineffective management [4]. Current treatments, such as thrombolysis and mechanical thrombectomy, aim to restore blood flow rapidly; however, their effectiveness is often limited by the narrow therapeutic window and the complexities involved in post-stroke recovery [5].

Recent research in ischemic stroke has increasingly focused on the role of central nervous system microglia [6]. A Study employing oxygen–glucose deprivation/reoxygenation (OGD/R) models have provided valuable insights into microglial responses during ischemic conditions [7]. Furthermore, research involving lipopolysaccharide (LPS) and interferon-gamma (IFN-γ) treatments has demonstrated their role in driving the M1 polarization of microglia, which is associated with pro-inflammatory responses and exacerbation of stroke pathology [8]. M1 microglia contribute to neuroinflammation and tissue damage, while M2 microglia, typically promoted under different conditions, are involved in tissue repair and resolution of inflammation [9]. Understanding the balance between these polarization states is crucial for developing targeted therapeutic strategies to modulate microglial activity. Despite ongoing advances in treatment, stroke prognosis re-

mains variable, with many patients experiencing persistent neurological deficits [10]. Thus, there is an urgent need for innovative diagnostic biomarkers and therapeutic interventions to enhance patient outcomes and mitigate the global burden of stroke.

Fc gamma receptor Ia (*FCGR1A*), also known as *CD64*, encodes a high-affinity receptor for the Fc portion of immunoglobulin G (IgG) and is predominantly expressed in monocytes, macrophages, and dendritic cells [11]. This receptor plays a pivotal role in mediating antibody-dependent cellular phagocytosis and inflammatory responses by facilitating the clearance of pathogens and activating pro-inflammatory pathways. Given its role in these processes, *FCGR1A* is recognized as a significant contributor to various inflammatory diseases. Weng W *et al*. [12] identify *FCGR1A* as crucial in peripheral immune activation and neuroinflammation in aneurysmal subarachnoid hemorrhage (aSAH), while Minett T *et al*. [13] link *FCGR1A* to microglial activation and Alzheimer's disease-related decrease in cognition. A recent analysis of datasets from ischemic stroke and non-alcoholic fatty liver disease (NAFLD) identified *FCGR1A*, among other genes, as a familiar immune-related candidate [14]. The AMP-activated protein kinase (AMPK)–mTOR pathway regulates cellular metabolism, growth, and stress responses and has also been implicated in modulating inflammatory processes. A study demonstrated this pathway's critical function in controlling neuroinflammation and microglia/macrophage polarization in cerebral ischemia–reperfusion injury [15]. Furthermore, Sun Z *et al*. [16] demonstrated that AMPK–mTOR signaling pathway activation can protect human umbilical cord mesenchymal stem cells (HUMSCs) from stroke-induced apoptosis and inflammation. These results highlight the possibility of focusing on the interplay between *FCGR1A* and the AMPK–mTOR pathway to develop novel therapeutic strategies for stroke and related diseases.

This study aims to elucidate the function of *FCGR1A* in ischemic stroke and its underlying processes in BV2 microglia. The effects of *FCGR1A* overexpression and knockdown, and mTOR inhibition on cellular inflammation and polarization were investigated to explore potential therapeutic targets for alleviating stroke-induced neuroinflammation. Our findings highlight *FCGR1A* as a key regulator of inflammatory processes and cellular phenotypic transitions, providing insights into new strategies for managing ischemic stroke and related neuroinflammatory conditions.

2. Materials and Methods

2.1 Downloading and Processing of the GSE58294 Dataset

The microarray dataset from GSE58294 was obtained from Gene Expression Omnibus (GEO, https://www.ncbi.nlm.nih.gov/gds/) and preprocessed by the R software (Version 4.0.3; R Foundation for Statistical Computing, Vienna, Austria). The dataset includes blood samples from cardiogenic stroke patients (n = 69) and control subjects (n = 23). The average expression value of these probe sets was computed for genes with multiple probe sets. Differential analysis was performed using the GEO2R tool after the probe IDs were converted to gene symbols. Fold change (FC) threshold >1 was called upregulated differentially expressed genes (DEGs), FC <1 was called downregulated DEGs, and the adjusted p-value threshold was <0.05.

2.2 Analysis of Protein–Protein Interactions (PPIs)

We conducted a network analysis utilizing the Search Tool for the Retrieval of Interacting Genes (STRING, https://string-db.org/) database to investigate PPI networks within the DEGs. The resulting network, which included clusters recognized by maximal neighborhood component (MNC) and molecular complex detection (MCODE), was shown with Cytoscape (Version 3.7.1; Institute for Systems Biology, Seattle, WA, USA), a platform for network visualization that is open-source. This allowed for a comprehensive examination of the interactions among proteins. The criterion for statistical significance was fixed at $p < 0.05$.

2.3 Identification and Expression Analysis of Overlapping Genes

The genes in the MCODE and MNC modules were cross-analyzed to acquire overlapping genes using the bioinformatics platform (https://bioinformatics.psb.ugent.be/webtools/Venn/). To evaluate the expression levels of overlapping genes, we used R for data processing and boxplot visualization and examined their expression in the case and regular groups of the GSE58294 dataset.

2.4 Cell Lines and Culture

Mouse microglia (BV2) were obtained from the National Collection of Authenticated Cell Cultures (Shanghai, China) and maintained in Dulbecco's Modified Eagle Medium (DMEM; Gibco; Thermo Fisher Scientific, Inc.; Waltham, MA, USA; cat. no. 11965) supplemented with 1% penicillin–streptomycin (Gibco; Thermo Fisher Scientific, Inc.; Waltham, MA, USA; cat. no. 15140122) and 10% fetal bovine serum (FBS; Gibco; Thermo Fisher Scientific, Inc.; Waltham, MA, USA; cat. no. 16000044). The temperature of the cell cultures was kept at 37 °C in a humidified environment with 5% CO_2.

2.5 Cell Treatment

OGD/R is a popular *in vitro* experimental method to simulate ischemia-reperfusion damage and investigate associated cellular protection mechanisms. The medium was replaced with D-glucose-free DMEM (Corning; Riverfront Plaza, Corning, NY, USA; cat. No. 17-207-CV) and incubated at 37 °C in a hypoxic incubator (94% nitrogen and 5% carbon dioxide) for 2 h to simulate OGD damage. The cells were transferred to a standard glucose-containing DMEM (Gibco; Thermo Fisher Scientific, Inc.; Waltham,

MA, USA; cat. no. 11965) medium in a regular incubator (reoxygenation). In this investigation, BV2 cells were given OGD/R conditions for 12, 24, and 48 hours to model ischemic injury. To induce an inflammatory response and promote M1 polarization, BV2 cells were treated with IFN-γ (MeilunBio; Dalian, Liaoning, China; cat. no. MB5954; 20 ng/mL) and LPS (Beyotime Biotechnology; Haimen, Jiangsu, China; cat. no. ST1470; 100 ng/mL) for 24 hours. Additionally, rapamycin (PAP; Beyotime Biotechnology; Haimen, Jiangsu, China; cat. no. S1842), an allosteric mTOR inhibitor, was administered at a concentration of 50 nM, and BV2 cells were treated for 24 hours to investigate its effects on cellular signaling pathways.

2.6 Transfection Assay

For transient transfection, a density of 2×10^5 cells per well was applied to seed BV2 cells in 24-well plates. Overexpression of *FCGR1A* in BV2 cells was performed by transfecting the cells with a plasmid encoding the *FCGR1A* gene. According to the manufacturer's protocol, transfections utilized Lipofectamine 3000 (Invitrogen; Thermo Fisher Scientific, Inc.; Carlsbad, CA, USA; cat. no. L3000). To knock down *FCGR1A* expression, BV2 cells were transfected with specific small interfering RNA (siRNA) targeting *FCGR1A*. After transfection, cells were cultured for 48 hours to allow for efficient overexpression or knockdown of *FCGR1A*. The sequence of si-*FCGR1A* is CGUUCAGAUCUCCACGCCUAGUUAU (sense Sequence); AUAACUAGGCGUGGAGAUCUGAACG (antisense Sequence). The sequence for small interfering RNA negative control (si-NC) is CGUUAGACCUCCGCAGAUCUCUUAU (sense Sequence); AUAACUAGGCGUGGAGAUCUGAACG (antisense Sequence).

2.7 Quantitative Real-Time Polymerase Chain Reaction (qRT-PCR)

The total RNA of BV2 cells was extracted using the TRIzol reagent (Tiangen; Xuhui District, Shanghai, China; Cat. no. 4992730) according to the manufacturer's instructions. To synthesize cDNA, we utilized a PrimeScript RT kit (Takara Biotechnology Co., Ltd.; Changping District, Beijing, China; cat. no. RR037). SYBR Green PCR Master Mix (Vazyme Biotech Co., Ltd.; Nanjing Economic and Technological Development Zone, Nanjing, China; cat. no. A0012) was applied for qRT-PCR via the StepOnePlus Real-Time PCR System (Applied Biosystems; Thermo Fisher Scientific, Inc.; Waltham, MA, USA). The levels of gene expression were measured and adjusted for GAPDH. The $2^{-\Delta\Delta CT}$ method was utilized to compute each target expression level. A primer sequence was set in Table 1.

Table 1. Primer sequences for qRT-PCR.

Target	Direction	Sequence (5′-3′)
FCGR1A	Forward	CTCACAGGGTGGATGGGTTC
FCGR1A	Reverse	CAAATCTGGGGAGGGTGCAT
CD16	Forward	GAGTCAGTCTGTCAGTCGGC
CD16	Reverse	GCCCCGAGTCTTGATTCGAT
CD32	Forward	GTACTATCTGCCAAGCCGGG
CD32	Reverse	CATGAGTCCCAGCAGCAAGA
iNOS	Forward	GGAGCGCTCTAGTGAAGCAA
iNOS	Reverse	TCCACTGCCCCAGTTTTTGA
CD206	Forward	GGCTGATTACGAGCAGTGGA
CD206	Reverse	ATGCCAGGGTCACCTTTCAG
Arg-1	Forward	ATCGGAGCGCCTTTCTCAAA
Arg-1	Reverse	CAGACCGTGGGTTCTTCACA
IL-10	Forward	CCAAGGTGTCTACAAGGCCA
IL-10	Reverse	ACGAGGTTTTCCAAGGAGTTGT
IL-1α	Forward	GAGCCGGGTGACAGTATCAG
IL-1α	Reverse	ACTTCTGCCTGACGAGCTTC
IL-1β	Forward	TGCCACCTTTTGACAGTGATGA
IL-1β	Reverse	GCCTGCCTGAAGCTCTTGTT
IL-6	Forward	TGATGGATGCTACCAAACTGGA
IL-6	Reverse	GTGACTCCAGCTTATCTCTTGG
TNF-α	Forward	CACACTCACAAACCACCAAGTG
TNF-α	Reverse	GCAGCCTTGTCCCTTGAAGA
TGF-β	Forward	CTCAGATGGGGCGCTCATAC
TGF-β	Reverse	AGAGCACACACAGGGATTGC
GAPDH	Forward	CCCTTAAGAGGGATGCTGCC
GAPDH	Reverse	ATGAAGGGGTCGTTGATGGC

qRT-PCR, quantitative real-time polymerase chain reaction; *FCGR1A*, Fc gamma receptor Ia; *CD16*, Fc gamma receptor IIIa; *Arg-1*, Arginase-1; *iNOS*, Inducible nitric oxide synthase; *IL*, interleukin; *TNF-α*, tumour necrosis factor-alpha; *TGF-β*, transforming growth factor β.

2.8 Western Blot (WB) Assay

Protease and phosphatase inhibitors (CoWin Biosciences; Taizhou, Jiangsu, China; cat. no. CW2200S) were added to radio-immunoprecipitation assay (RIPA) lysis buffer (Solarbio; Tongzhou Dist, Beijing, China; cat. no. R0010) to obtain protein lysates from BV2 cells. The bicinchoninic acid (BCA) Protein Assay Kit (Beyotime Biotechnology; Haimen, Jiangsu, China; cat. no. P0009) was applied to measure the protein concentration. Polyvinylidene fluoride membranes (PVDF; Beyotime Biotechnology; Haimen, Jiangsu, China; cat. no. FFP22) were utilized to receive equal quantities of protein that had been separated with 10% Sodium dodecyl sulfate polyacrylamide gel electrophoresis (SDS-PAGE). Membranes were blocked with 5% skim milk and then incubated with primary antibodies against FCGR1A (cat. no. ab140779), interleukin (IL)-6 (cat. no. ab233706), induction of brown adipocytes 1 (Iba1) (cat. no. ab178847), FC gamma receptor IIIa (CD16) (cat. no. ab246222), inducible nitric oxide synthase (iNOS) (cat. no. ab178945), CD206 (cat. no. ab64693), Arginase-1 (Arg-1) (cat. no. ab133543), p-AMPK (cat. no. ab133448), AMPK (cat. no. ab32047), p-mTOR (cat. no. ab109268), and mTOR (cat. no.

ab32028) (all from Abcam, Cambridge, MA, USA). Except for FCGR1A, which was diluted at a ratio of 1:4000, all other antibodies were diluted at a ratio of 1:1000. Membranes were cleaned and then treated with the relevant secondary antibodies, including goat anti-rabbit IgG-HRP (cat. no. ab6721; dilution 1:5000) and goat anti-mouse IgG-HRP (cat. no. ab6789; dilution 1:5000) (all from Abcam, Cambridge, MA, USA). GAPDH (Kangcheng; Caohejing Hi-Tech Development Zone, Shanghai, China; cat. no. KC-5G4; 1:5000) was an internal reference. A Chemi-Doc imaging system (Bio-Rad, Shanghai, China; cat. no. 12003153) was employed to obtain the images of the protein bands, which were viewed using an enhanced chemiluminescence (ECL) kit (Tiangen; Xuhui District, Shanghai, China; cat. no. ZN1926).

2.9 Enzyme-Linked Immunosorbent Assay (ELISA)

Samples of cell culture supernatant were appropriately diluted and put into the wells of an ELISA plate that had been coated beforehand with tumor necrosis factor-alpha (TNF-α) (Invitrogen; Thermo Fisher Scientific, Inc.; Carlsbad, CA, USA; cat. no. BMS607-3), IL-1β (Invitrogen; Thermo Fisher Scientific, Inc.; Carlsbad, CA, USA; cat. no. BMS6002-2), IL-10 (Invitrogen; Thermo Fisher Scientific, Inc.; Carlsbad, CA, USA; cat. no. BMS614), and IL-6 (Invitrogen; Thermo Fisher Scientific, Inc.; Carlsbad, CA, USA; cat. no. BMS603-2)-specific antibodies. Following incubation, plates were washed to remove unbound material. Enzyme-linked secondary antibodies were added to each well, after which a chromogenic substrate was added. The response was terminated using an appropriate stop solution, and absorbance was detected at the specific wavelength recommended for the substrate utilizing a microplate reader. By comparing the absorbance readings to a standard curve created from standards of known quantities, the amounts of TNF-α, IL-1β, IL-10, and IL-6 were determined.

2.10 Immunofluorescence Staining

Cells or tissue sections were fixed with 4% paraformaldehyde (Beyotime Biotechnology; Haimen, Jiangsu, China; cat. no. PFA; P0099) at room temperature for 15 minutes. Following fixation, samples were permeabilized with 0.2% Triton X-100 (Bioss; Tongzhou District, Beijing, China; cat. no. C03-02002) for 10 minutes. To reduce non-specific binding, samples were stopped utilizing 5% BSA (Solarbio; Tongzhou Dist, Beijing, China; cat. no. SW3015) in PBS for 1 hour. The samples were treated with primary antibodies diluted in 1% BSA in PBS and incubated at 4 °C for a whole night. The primary antibodies used were Iba1 (cat. no. ab178847, dilution 1:100), FCGR1A (cat. no. ab140779, dilution 1:100), CD16/32 (cat. no. ab25235, dilution 1:200), and CD206 (cat. no. ab64693, dilution 1:100) (all from Abcam, Cambridge, MA, USA). After washing with PBS, samples were incubated with fluorescent dye-conjugated secondary antibodies, including goat anti-rabbit IgG Alexa Fluor® 488 (cat. no. ab150077, dilution 1:500) and goat anti-mouse IgG Alexa Fluor® 594 (cat. no. ab150116, dilution 1:500) (all from Abcam, Cambridge, MA, USA) at room temperature for 1 hour. DAPI (Invitrogen; Thermo Fisher Scientific, Inc.; Carlsbad, CA, USA; cat. no. D1306) was applied as a five-minute counterstain on the nuclei. Finally, samples were elevated using Fluoromount-G (Yeasen, Shanghai, China; cat. no. 36307ES) and pictured using a confocal microscope (FV1000, Olympus, Beijing, China), magnification 20×. Images were captured and analyzed with ZEN software (Version 3.1, Zeiss, Oberkochen, Germany).

2.11 Statistical Analysis

R software was employed to conduct statistical analysis. Data from experiments carried out thrice are displayed as mean ± standard deviation (SD) [17]. An independent *t*-test was employed to compare the two groups. Tukey's posthoc test was applied to determine specific group differences in comparisons involving several groups, after which a one-way ANOVA was conducted. A *p*-value of less than 0.05 was statistically significant.

2.12 Mycoplasma Detection Statement

In this study, we followed strict standard operating procedures for cell culture and assays to ensure the quality and authenticity of the cell lines used. The cells we used, BV2, were obtained from the National Center for the Preservation of Certified Cell Cultures. To further validate these cell lines' authenticity and rule out the possibility of mycoplasma contamination, we performed mycoplasma testing on all cell lines. The assay results showed no mycoplasma contamination was detected in any of the cell lines tested, and all results were negative (**Supplementary Fig. 1**). While STR profiling was not independently performed in our lab, STR reference data are available from the supplier (https://www.cellbank.org.cn/search-detail.php?id=899), and the cell line has not been reported to be misidentified or contaminated. We are committed to complying with scientific and ethical standards for all cell lines used in our research, and we will continue to monitor and maintain the integrity of our cell lines.

3. Results

3.1 DEG Screening and Expression Analysis in Stroke

A total of 197 downregulated and 130 upregulated DEGs were found in the GSE58294 dataset, comprising 23 control and 69 cardioembolic stroke samples (Fig. 1A). Through the STRING database, PPI network analysis of these DEGs revealed a network with 164 nodes and 302 edges. The MCODE algorithm identified a subnetwork containing 12 nodes and 24 edges, while the MNC algorithm identified a subnetwork with 10 nodes and 22

edges (Fig. 1B,C). Five overlapping genes (catenin beta 1 (*CTNNB1*), SRY-box transcription factor 9 (*SOX9*), matrix metallopeptidase 9 (*MMP9*), CD19 molecule (*CD19*), and *FCGR1A*) were identified using the bioinformatics platform from the MCODE and MNC subnetworks (Fig. 1D). Expression analysis indicated that *CTNNB1*, *MMP9*, and *FCGR1A* were upregulated in the stroke samples, whereas *SOX9* and *CD19* were upregulated in the non-stroke control samples within the GSE58294 dataset (Fig. 1E and **Supplementary Table 1**). *FCGR1A* plays a role in the immune system, helping to clear damaged tissue and control inflammation, which is essential for stroke recovery. *FCGR1A* may work by affecting the activity and movement of immune cells, affecting inflammation and repair processes after stroke. The increase in *FCGR1A* in stroke patient samples in the GSE58294 dataset may indicate its role in the early stages of stroke, which may be in response to ischemic injury. *FCGR1A* was bioinformatically associated with ischemic stroke in a previous study [14]. Still, its detailed functional role and mechanism in stroke have not been fully explored and deserve further study, so we chose it as a hub gene.

3.2 Time-Dependent Upregulation of FCGR1A and IL-6 in BV2 Cells Induced by OGD/R

WB analysis was conducted to evaluate the protein levels of FCGR1A in BV2 cells exposed to 12, 24, and 48 hours of OGD/R. The results demonstrated a time-dependent increase in FCGR1A protein expression, with higher levels observed at longer treatment durations (Fig. 2A,B). In addition, we used immunofluorescence staining to detect the expression of FCGR1A and Iba1, which are specific markers for microglia and macrophages and whose expression plays a role in microglia activation and polarization. Immunofluorescence results showed enhanced fluorescence signals of FCGR1A and Iba1 in BV2 cells after 24 hours of reoxygenation, indicating increased FCGR1A activation (Fig. 2C). These observations suggest that FCGR1A is activated in response to OGD/R-induced injury. Furthermore, the protein levels of IL-6 in BV2 cells increased progressively with OGD/R treatment durations of 0, 12, 24, and 48 hours, as shown by WB analysis (Fig. 2D,E).

3.3 FCGR1A Overexpression Induces an Inflammatory Response and Promotes M1 Polarization in BV2 Cells

The effectiveness of *FCGR1A* overexpression in BV2 cells was confirmed by qRT-PCR and WB methods (Fig. 3A–C). The levels of pro-inflammatory cytokines in BV2 cells were calculated using the ELISA method after treatment with LPS+IFN-γ or *FCGR1A* overexpression. The outcomes demonstrated that the expression of these cytokines enhanced significantly after treatment (Fig. 3D–F), indicating that *FCGR1A* contributes to the activation of inflammatory response in BV2 cells. In addition, qRT-PCR analysis demonstrated that both LPS+IFN-γ stimulation and *FCGR1A* overexpression significantly increased M1 polarization markers *CD32*, *CD16*, and *iNOS* (Fig. 3G–I). In contrast, the M2 markers Arg-1, IL-10, and CD206 levels under the same conditions were not significantly affected (Fig. 3J–L). These findings suggest that *FCGR1A* promotes inflammatory responses and enhances M1 polarization in BV2 cells.

3.4 FCGR1A Knockdown Attenuates OGD/R-Induced Inflammatory Response in BV2 Cells

The knockdown efficiency of *FCGR1A* in BV2 cells was verified using qRT-PCR and WB analysis (Fig. 4A–C). Subsequent qRT-PCR analysis under OGD/R treatment conditions showed that silencing *FCGR1A* significantly reduced the mRNA expression levels of *IL-1*β, *IL-1*α, *TNF-*α, and *IL-6* (Fig. 4D–G). Conversely, the mRNA expression of transforming growth factor β (*TGF-*β) and *IL-10* were markedly upregulated after *FCGR1A* knockdown (Fig. 4H,I). These results indicate that the knockdown of *FCGR1A* reduces the inflammatory reactions in BV2 cells and encourages the expression of anti-inflammatory cytokines under OGD/R-induced stress conditions.

3.5 FCGR1A Knockdown Reduces Inflammatory Response and Promotes M2 Polarization in BV2 Cells Following OGD/R Treatment

The expression of M1 markers (CD16 and CD32) and M2 markers (CD206) in BV2 cells following OGD/R therapy and *FCGR1A* knockdown was assessed by immunofluorescence labeling. CD16/32 is usually associated with M1-type microglia, whereas CD206 is with M2-type microglia. Differences in the expression of Iba1, CD16/32, and CD206 reveal the polarization characteristics of microglia in different states. The results showed that the number of Iba1-positive microglia/macrophages expressing M1 markers CD16 and CD32 was significantly reduced in *FCGR1A* knockdown cells compared with cells only exposed to OGD/R. Conversely, the number of cells expressing M2 marker CD206 increased, indicating a shift from M1 to M2 phenotype (Fig. 5A). Further qRT-PCR analysis showed that *FCGR1A* knockdown significantly elevated the levels of M2 polarization markers and reduced the levels of M1 polarization markers compared with the OGD/R group (Fig. 5B–F). ELISA results revealed that IL-10 was elevated and IL-1β was markedly decreased after *FCGR1A* knockdown compared with OGD/R treatment alone (Fig. 5G,H). WB analysis confirmed these findings, and the Iba1, CD16, and iNOS protein levels were considerably decreased, while Arg-1 and CD206 levels were raised in the *FCGR1A* knockdown group in contrast to the OGD/R group alone (Fig. 5I,J). These results suggest that *FCGR1A* knockdown promotes the transition of BV2 cells to the anti-inflammatory M2 phenotype, thereby alleviating OGD/R-induced inflammation.

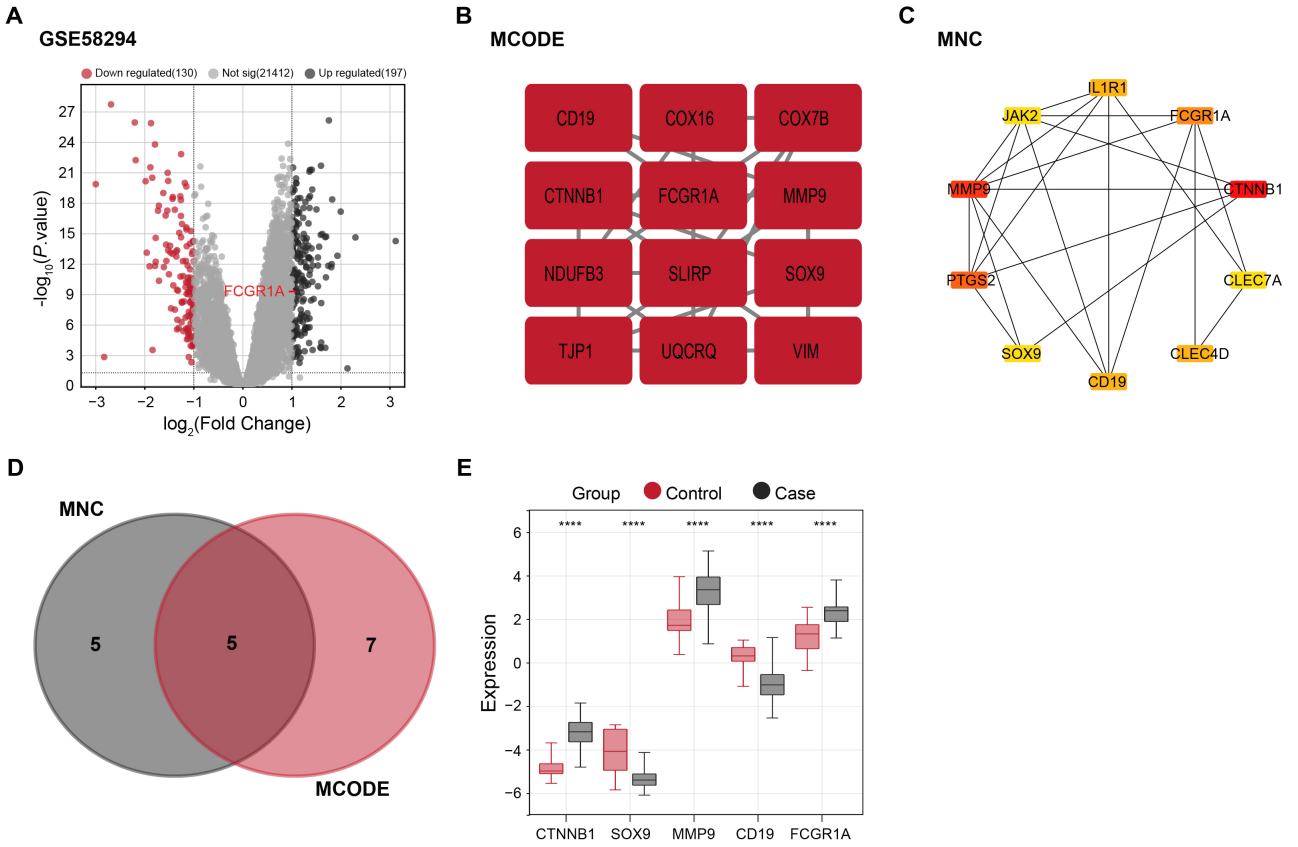

Fig. 1. Identification of DEGs and selection of hub genes in the GSE58294 dataset. (A) Volcano plot of DEG screening results in the GSE58294 dataset. Red represents upregulated DEGs, black represents downregulated DEGs, and gray represents genes with insignificant expression. (B,C) PPI network analysis of DEGs, including MCODE (B) and MNC (C) algorithms. The MCODE algorithm contains 12 nodes and 24 edges, and the MNC algorithm includes 10 and 22 edges. Nodes represent proteins or protein domains, and edges represent interactions between these proteins. (D) Venn diagram of 5 overlapping genes in MCODE and MNC, including *CTNNB1*, *SOX9*, *MMP9*, *CD19*, and *FCGR1A*. (E) Analysis of overlapping gene expression in non-stroke control and stroke samples of the GSE58294 dataset. Red represents the control sample, and black represents the case sample. DEGs, differentially expressed genes; PPI, protein–protein interaction; MCODE, molecular complex detection; MNC, maximal neighborhood component; *CTNNB1*, catenin beta 1; *SOX9*, SRY-box transcription factor 9; *MMP9*, matrix metallopeptidase 9. ****$p < 0.0001$.

3.6 FCGR1A Regulates the AMPK–mTOR Pathway to Promote the Transition of BV2 Cells to the M2 Phenotype

Rapamycin (RAP), a well-known mTOR inhibitor, was applied to BV2 cells subjected to OGD/R. WB analysis revealed that both si-*FCGR1A* and 50 nM RAP treatment significantly increased p-AMPK protein levels while decreasing p-mTOR protein levels compared to OGD/R treatment alone, with no notable alterations in total AMPK and mTOR protein expression. The combination of si-*FCGR1A* and RAP further amplified these effects (Fig. 6A,B). qRT-PCR analysis demonstrated that M1 polarization markers expression was significantly reduced, while M2 polarization markers were correspondingly increased following si-*FCGR1A* or RAP treatment. These changes were even more pronounced when the two interventions were combined (Fig. 6C–G). ELISA results showed that both si-*FCGR1A* and RAP treatment led to a rise in the anti-inflammatory cytokine and a significant decline in the pro-inflammatory cytokine, with a more substantial effect observed with combined treatment (Fig. 6H,I). WB analysis further confirmed these findings, showing a marked decrease in Iba1 and the M1 marker CD16 and a significant increase in CD206 in cells treated with either si-*FCGR1A* or RAP, with more pronounced changes following the combined treatment (Fig. 6J,K). These findings suggest that under OGD/R conditions, *FCGR1A* knockdown and mTOR inhibition synergistically enhance AMPK activation, leading to the promotion of M2 polarization and suppression of M1 polarization in BV2 cells.

4. Discussion

Worldwide, ischemic stroke accounts for the majority of stroke cases, making it a primary cause of mortality and disability [18]. Identifying the molecular mechanisms involved in stroke can provide insights into potential therapeutic targets. This study's bioinformatics analysis

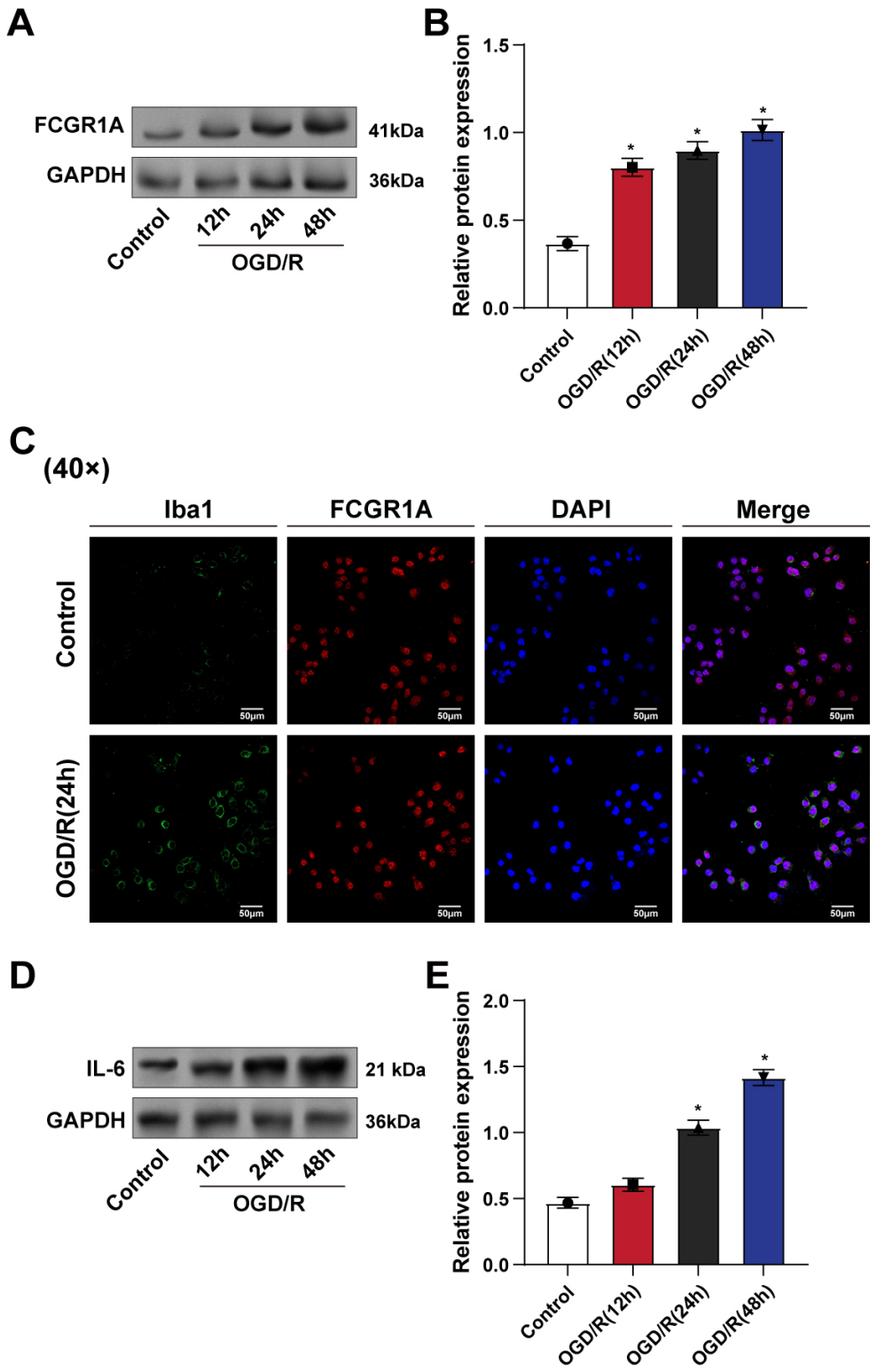

Fig. 2. Time-dependent upregulation of *FCGR1A* and IL-6 in BV2 cells after OGD/R treatment. (A,B) WB detection of FCGR1A protein level in BV2 cells after OGD/R treatment for 12 h, 24 h, and 48 h. (C) Iba1 (green) and FCGR1A (red) protein expressions in BV2 cells were detected by immunofluorescence after 24 h of OGD/R treatment. (D,E) WB detection of inflammatory factor IL-6 protein level in BV2 cells after OGD/R treatment (12, 24, 48 h). WB, Western blot; OGD/R, oxygen–glucose deprivation/reoxygenation; Iba1, induction of brown adipocytes 1. *$p < 0.05$. Original magnification: 20×. Scale, 50 μm. Statistical plots of WB experiments represent the SD ± mean of a single occasion, and immunofluorescence experiments were performed with at least three independent replicates.

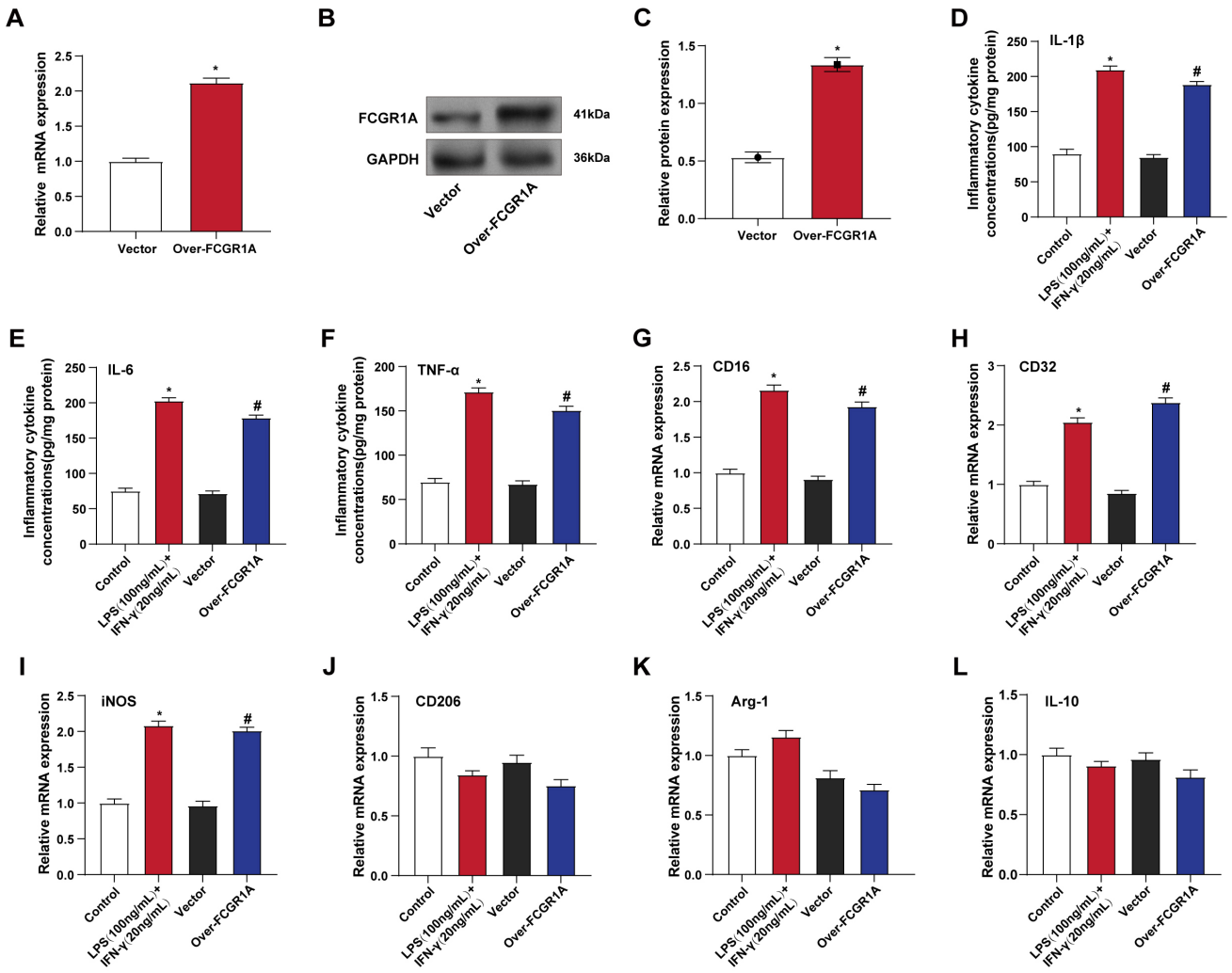

Fig. 3. *FCGR1A* overexpression induces inflammatory responses and promotes M1 polarization in BV2 cells. (A–C) qRT-PCR (A) and WB (B,C) were used to detect the efficiency of *FCGR1A* overexpression in BV2 cells. *$p < 0.05$. (D–F) ELISA was used to detect the concentration changes of inflammatory factors IL-1β (D), IL-6 (E), and TNF-α (F) in BV2 cells after LPS+IFN-γ or over-*FCGR1A*. *$p < 0.05$ vs. control. #$p < 0.05$ vs. vector. (G–L) qRT-PCR was used to detect the expression levels of M1 polarization markers (CD16 (G), CD32 (H), and iNOS (I)) and M2 polarization markers (CD206 (J), Arg-1 (K), and IL-10 (L)) in BV2 cells after LPS+IFN-γ or over-*FCGR1A* treatment. *$p < 0.05$ vs. control. #$p < 0.05$ vs. vector. qRT-PCR stands for quantitative real-time polymerase chain reaction; WB stands for Western blot; and ELISA stands for enzyme-linked immunosorbent assay. Statistical plots for WB experiments represent the SD $\pm$ mean of one trial, and statistical plots for qPCR and ELISA experiments represent the SD $\pm$ mean of at least three independent replicates. ELISA, enzyme-linked immunosorbent assay; LPS, lipopolysaccharide; IFN-γ, interferon-gamma.

of the GSE58294 dataset revealed five overlapping genes: *CTNNB1*, *SOX9*, *MMP9*, *CD19*, and *FCGR1A*. Our results showed that *CTNNB1*, *MMP9*, and *FCGR1A* were significantly upregulated in stroke samples, while *SOX9* and *CD19* were downregulated. Zhao XY *et al.* [19] identified that the *CTNNB1* polymorphism rs2953 increases stroke risk in the Chinese Han population by reducing *CTNNB1* mRNA expression through miR-3161 binding. Xu X *et al.* [20] demonstrated that *SOX9* limits post-stroke recovery by upregulating CSPG production, with *SOX9* knockout mice showing enhanced axonal sprouting and improved neurological outcomes, suggesting *SOX9* inhibition as a potential therapeutic strategy. Meanwhile, Zielińska-Turek J *et al.* [21] found that elevated *MMP-9* levels, coupled with reduced *TIMP* activity, are predictors of stroke risk and restenosis in patients with carotid stenosis undergoing stenting or endarterectomy. Although some bioinformatics studies have indicated that *FCGR1A* may be connected to ischemic stroke, its specific function and mechanism in stroke remain unclear. Therefore, we chose *FCGR1A* as a hub gene for further investigation in this study to elucidate its potential role in stroke pathology.

OGD/R is a typical model for ischemic stroke simulation and evaluating microglial responses *in vitro* [22]. This

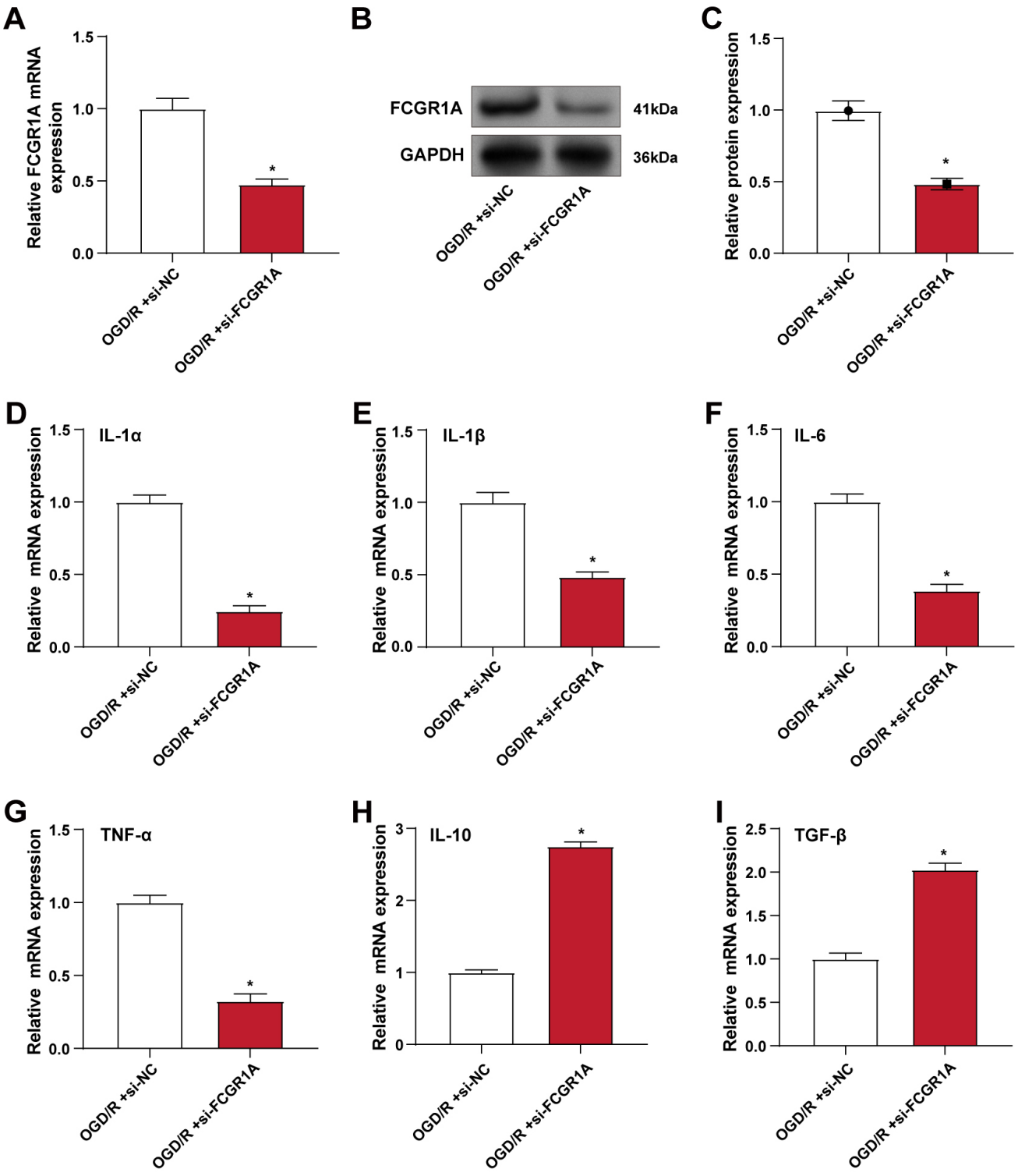

Fig. 4. Knockdown of *FCGR1A* alleviates OGD/R-induced inflammatory response in BV2 cells. (A–C) qRT-PCR (A) and WB (B,C) were used to detect the knockdown efficiency of *FCGR1A* in BV2 cells under OGD/R conditions. (D–I) qRT-PCR was used to detect the changes in the mRNA levels of pro-inflammatory factors *IL-1α* (D), *IL-1β* (E), *IL-6* (F), and *TNF-α* (G) and anti-inflammatory factors *IL-10* (H) and *TGF-β* (I) in BV2 cells after 24 h of OGD/R treatment. qRT-PCR, quantitative real-time polymerase chain reaction; WB, Western blot; OGD/R, oxygen–glucose deprivation/reoxygenation; si-NC, small interfering RNA negative control. *$p < 0.05$. Statistical plots of WB experiments represent the SD ± mean of a single run, and statistical plots of qPCR experiments were performed with the SD ± mean of at least three independent replicates.

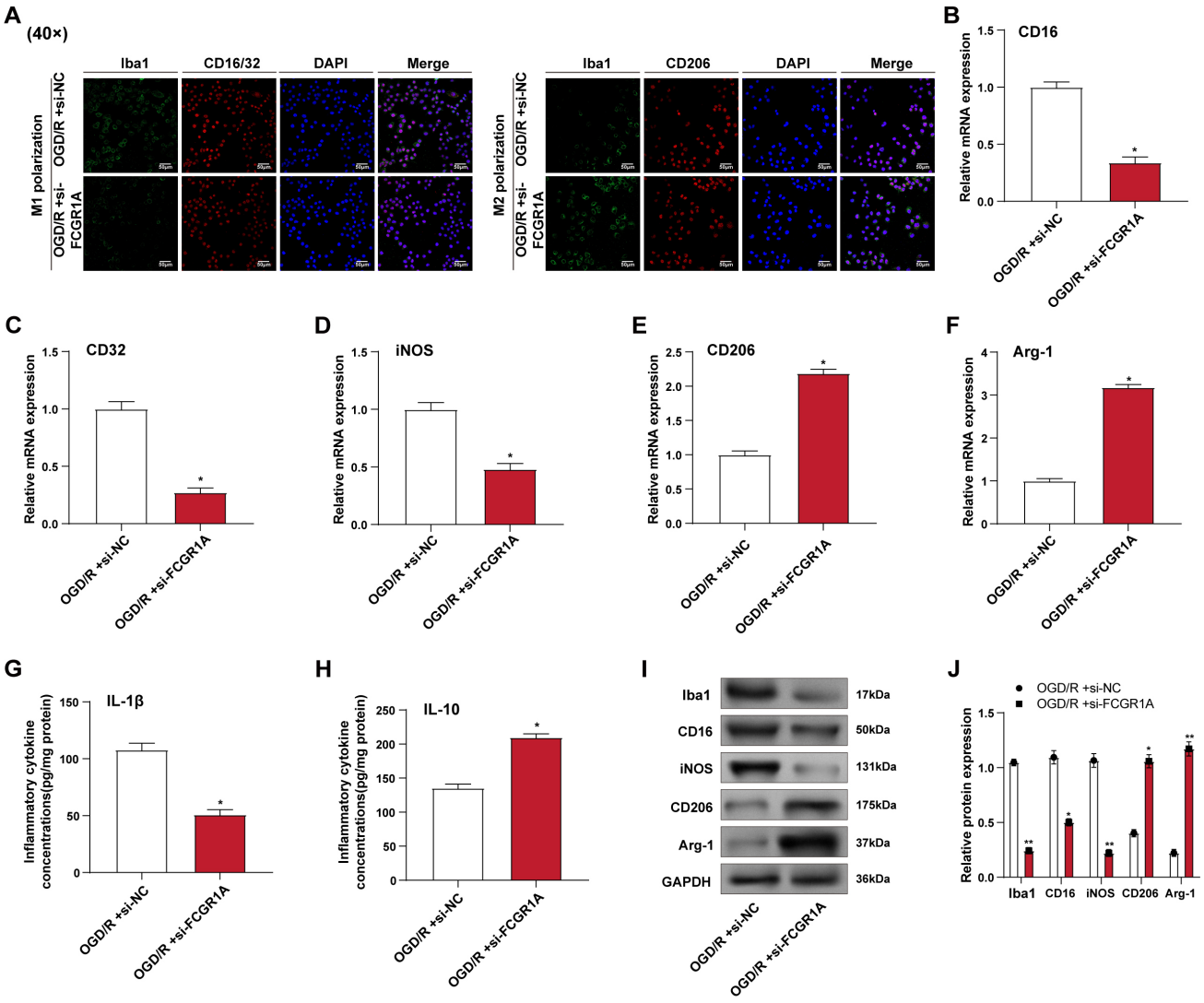

Fig. 5. *FCGR1A* knockdown promotes the transition of BV2 cells from M1 to M2 phenotype after OGD/R treatment. (A) Immunofluorescence staining of BV2 cells for Iba1, M1 markers (CD16, CD32), and M2 marker (CD206) after OGD/R and *FCGR1A* knockdown. (B–F) qRT-PCR detection of the mRNA levels of M1 polarization markers CD16 (B), CD32 (C) and iNOS (D), M2 markers CD206 (E) and Arg-1 (F) in BV2 cells after OGD/R and *FCGR1A* knockdown. (G,H) ELISA detection of the protein concentrations of M1 polarization inflammatory factor IL-1β and M2 polarization inflammatory factor IL-10 in BV2 cells after OGD/R and *FCGR1A* knockdown. (I,J) WB analysis of Iba1, CD16, iNOS, CD206, and Arg-1 protein levels in BV2 cells after OGD/R and *FCGR1A* knockdown. qRT-PCR, quantitative real-time polymerase chain reaction; WB, Western blot; ELISA, enzyme-linked immunosorbent assay; OGD/R, oxygen–glucose deprivation/reoxygenation. *$p < 0.05$. **$p < 0.01$. Original magnification: 20×. Scale, 50 µm. Statistical plots of WB experiments represent the SD ± mean of a single run, statistical plots of qPCR experiments and ELISA experiments were carried out with at least three independent replicates of the SD ± mean, and immunofluorescence experiments were carried out with at least three independent replicates.

treatment induces a stress response in microglia, characterized by heightened inflammation and activation, which is critical for understanding stroke pathophysiology. In our study, OGD/R treatment increased inflammation in BV2 cells, as indicated by elevated Iba1 and IL-6 levels. Increased Iba1 is associated with more severe stroke and poorer outcomes, highlighting its clinical relevance. IL-6 is a prognostic marker in ischemic stroke, with higher levels linked to cognitive dysfunction, suggesting its role not only in stroke onset but also in post-stroke recovery and cognitive impairment—an integrative review: challenges [23]. LPS, a component of Gram-negative bacterial membranes, triggers a strong immune response, leading to pro-inflammatory cytokine production. IFN-γ is a cytokine that enhances inflammatory responses and immune regulation. LPS and IFN-γ synergistically activate macrophages and microglia, promoting M1 polarization and increasing pro-inflammatory mediator produc-

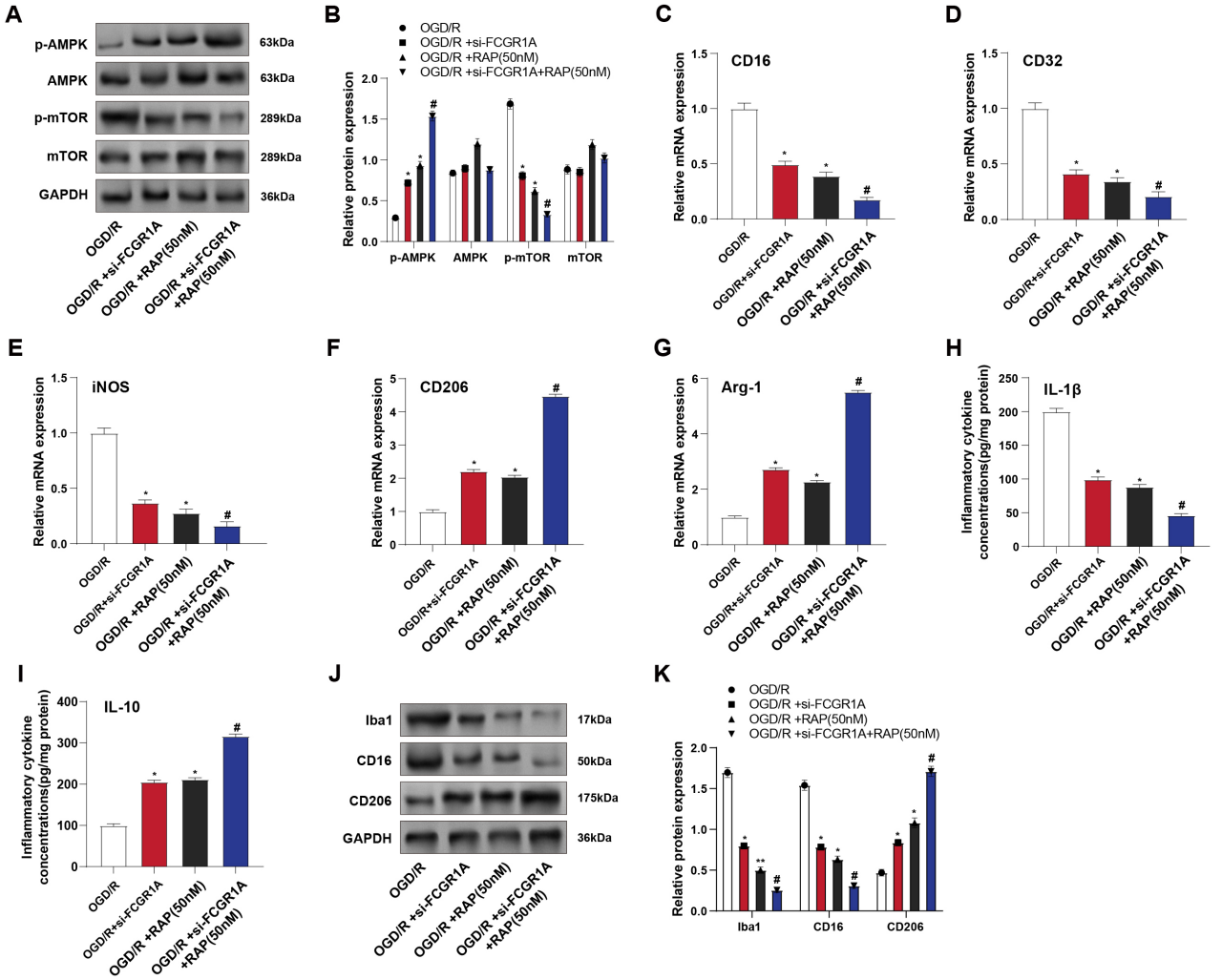

Fig. 6. *FCGR1A* regulates the AMPK–mTOR signaling pathway to promote the transition of BV2 cells to the M2 phenotype. (A,B) WB detected the levels of proteins related to the AMPK–mTOR signaling pathway in BV2 cells after OGD/R, si-*FCGR1A*, and RAP (mTOR inhibitor) treatment. (C–G) qRT-PCR detected the mRNA levels of M1 polarization markers *CD16* (C), *CD32* (D), and *iNOS* (E) and M2 markers *CD206* (F) and *Arg-1* (G) in BV2 cells after OGD/R, si-*FCGR1A* and RAP treatment. (H,I) ELISA detected the protein concentrations of M1 polarization pro-inflammatory factor IL-1β (H) and M2 polarization anti-inflammatory factor IL-10 (I) in BV2 cells after OGD/R, si-*FCGR1A*, and RAP treatment. (J,K) WB analysis of Iba1, CD16, and CD206 protein levels in BV2 cells after OGD/R, si-*FCGR1A*, and RAP treatment. AMPK, AMP-activated protein kinase; qRT-PCR, quantitative real-time polymerase chain reaction; WB, Western blot; ELISA, enzyme-linked immunosorbent assay; OGD/R, oxygen–glucose deprivation/reoxygenation; RAP, rapamycin. *$p < 0.05$, **$p < 0.01$ vs. OGD/R. #$p < 0.05$ vs. OGD/R+si-*FCGR1A*. Statistical plots for WB experiments represent the SD $\pm$ mean of one trial, and statistical plots for qPCR and ELISA experiments represent the SD $\pm$ mean of at least three independent replicates.

tion. Wu CC *et al.* [24] showed that this combination induces pro-inflammatory microglial polarization and neuronal degeneration in a stroke model. At the same time, β-funaltrexamine reduces these effects by promoting an anti-inflammatory state. Similarly, Yang C *et al.* [25] found that LPS and IFN-γ lead to pro-inflammatory microglial polarization and neuronal damage. These findings underscore the role of inflammation and microglial polarization in stroke pathology and the potential for therapeutic intervention.

Microglial polarization is intricately linked to stroke outcomes, with M1 polarization exacerbating inflammation and neuronal damage, while M2 polarization supports tissue repair and neuroprotection [26]. Recent studies have highlighted various mechanisms influencing microglial polarization in ischemic stroke. Zou J *et al.* [27] reported that electroacupuncture (EA) enhances M2 polarization through annexin A1 (ANXA1) upregulation, reducing neuroinflammation and improving neurological outcomes. Conversely, Zhou X *et al.* [28] identified that

chemokine-like-factor 1 (CKLF1) upregulation in neurons drives M1 polarization, exacerbating neuroinflammation and neuronal damage, with NF-κB regulation of this process. Our study extends these findings, showing that *FCGR1A* upregulation enhances inflammation and encourages BV2 cells to become M1 polarized under OGD/R circumstances. We observed that *FCGR1A* overexpression increased pro-inflammatory cytokine levels and M1 markers, whereas *FCGR1A* knockdown reduced inflammation, decreased M1 markers, and facilitated a shift to the anti-inflammatory M2 phenotype. These results highlight the intricate function of microglial polarization in stroke pathology and suggest that *FCGR1A* might be a viable target for modulating inflammation and enhancing stroke outcomes.

The AMPK–mTOR pathway regulates cellular energy homeostasis and growth. AMPK senses cellular energy status and, when activated, inhibits the mTOR pathway to conserve energy. AMPK activation can suppress excessive neuronal growth and inflammation in ischemic stroke by downregulating mTOR signaling [29]. This modulation helps maintain cellular metabolism and protect neurons from damage. Moreover, AMPK activation promotes autophagy, a process essential for removing damaged cellular components, further aiding in neuroprotection and recovery post-stroke [30]. Recent investigations have demonstrated the critical function of the AMPK–mTOR signaling pathway in stroke management. Zhao M *et al*. [31] showed that metformin reduces oxidative stress and enhances neurological function in individuals suffering from acute stroke with type 2 diabetes by modulating this pathway, thereby improving neuroprotection and recovery. Yuan Y *et al*. [32] showed that kaempferol protects against harm from cerebral ischemic–reperfusion by activating the AMPK–mTOR signaling pathway, which induces autophagy, reduces neuronal apoptosis, and improves outcomes in a rat stroke model. Conversely, Wang L *et al*. [33] found that epigallocatechin-3-gallate (EGCG) mitigates harm from ischemia–reperfusion by inhibiting autophagy through the AKT/AMPK/mTOR cascade, leading to reduced infarct volume and neuronal loss in both mouse models and *in vitro* cell cultures. Similar to the above studies, this research found using *in vitro* cell experiments that under OGD/R conditions, *FCGR1A* knockdown and mTOR inhibition synergistically enhanced AMPK activation, resulting in the inhibition of M1 polarization and the promotion of M2 polarization in BV2 cells, that is, *FCGR1A* regulates the AMPK–mTOR pathway and promotes the change of BV2 cells to the M2 phenotype. This suggests that dysregulation of the AMPK–mTOR pathway may lead to adverse consequences, highlighting its capacity as a target for therapy for improving stroke recovery and minimizing neuronal damage.

FCGR1A, a high-affinity IgG Fc receptor expressed on macrophages and monocytes, is key in regulating immune responses and inflammatory processes. Our findings that the expression level of *FCGR1A* was significantly upregulated in microglia under *in vitro* simulated ischemic conditions echoed the upregulation of *FCGR1A* in peripheral blood, suggesting that *FCGR1A* may play an essential role in the inflammatory response in stroke. Our findings support a functional role for *FCGR1A* in microglia polarization, particularly in promoting M1-type inflammatory responses and inhibiting M2-type anti-inflammatory responses. This was further confirmed by *FCGR1A* overexpression and knockdown experiments, in which upregulation of *FCGR1A* promoted inflammatory factor production and M1-type microglia polarization. In contrast, the downregulation of *FCGR1A* reduced inflammation and promoted M2-type anti-inflammatory polarization. These findings are consistent with previous studies that point to a role for *FCGR1A* in various inflammatory diseases and emphasize its potential importance in CNS inflammation. In addition, our study explored how *FCGR1A* regulates microglia polarization by affecting the AMPK–mTOR signaling pathway, which plays a central role in cellular metabolism, growth, and stress responses and whose role in regulating neuroinflammation and microglia/macrophage polarization in cerebral ischemia–reperfusion injury has been extensively studied. Our experimental results suggest that downregulation of *FCGR1A* in combination with the mTOR inhibitor RAP synergistically enhances AMPK activation, thereby promoting anti-inflammatory polarization of microglia toward the M2 type. This finding opens the possibility of developing new therapeutic strategies to attenuate the inflammatory response after stroke and promote neural repair by targeting *FCGR1A* and its associated signaling pathways.

A limitation of this study is that all experiments were performed *in vitro* using BV2 cells, which may not fully mimic the complex environment of ischemic stroke *in vivo*. Although BV2 cells provide a valuable model for studying the inflammatory response of microglial cells, they may not fully represent human microglial cell behavior. In addition, *in vitro* experimental conditions differ from the *in vivo* environment, such as cell–cell interactions, the composition of the extracellular matrix, and hemodynamics, which play an essential role in the *in vivo* stroke environment. Therefore, our findings need to be further validated by *in vivo* models in future studies to assess the accuracy of the therapeutic potential of *FCGR1A* in ischemic stroke. Furthermore, although our study revealed a role for *FCGR1A* in microglia polarization and provided strong evidence for a potential role of *FCGR1A* in ischemic stroke, there are still limitations that need to be further explored, especially about other possible mechanisms of *FCGR1A*'s role in poststroke inflammatory responses. Future studies should cover the analysis of *FCGR1A* expression patterns in stroke patient samples and assess the efficacy of *FCGR1A*-targeted therapies in stroke models.

5. Conclusion

This study identifies *FCGR1A* as a critical regulator of inflammation and microglial polarization in the context of ischemic stroke. Bioinformatics analysis showed that *FCGR1A* is a hub gene associated with stroke pathology. Experimental results demonstrated that *FCGR1A* overexpression in BV2 cells promotes M1 polarization and enhances inflammatory responses following OGD/R. Conversely, *FCGR1A* knockdown alleviates inflammation and facilitates the transition from M1 to M2 phenotype, indicating an anti-inflammatory shift. Notably, *FCGR1A* knockdown, combined with mTOR inhibition, synergistically activates the AMPK pathway, further promoting M2 polarization. These outcomes highlight the function of *FCGR1A* in regulating the AMPK–mTOR pathway and suggest its possibility as an intended treatment for adjusting inflammatory responses and improving outcomes in ischemic stroke.

Availability of Data and Materials

The datasets used and/or analyzed during the current study are available from the corresponding author upon reasonable request.

Author Contributions

ML, XF, DC, and YY designed the research study. HY, ZH, and HL performed the experiments. QZ, YW, and HS provided technical guidance and assistance with data collection. HS, ML, and DC analyzed the data. YY, XF, HY supervised the project and revised the manuscript. All authors contributed to editorial revisions, read and approved the final manuscript, and agreed to be accountable for all aspects of the work.

Ethics Approval and Consent to Participate

Not applicable.

Acknowledgment

Not applicable.

Funding

This study was funded by Shanghai Jinshan District Medical Key Specialty Construction Project Seventh Cycle (JSZK2023B01), and Jinshan Hospital Affiliated to Fudan University Reserve Discipline Platform Construction Project (HBXK-2022-4).

Conflict of Interest

The authors declare no conflict of interest. Although the author Haihan Song is from Shanghai Cyan Medical Co., Ltd., the judgments in data interpretation and writing were not influenced by this relationship.

Declaration of AI and AI-assisted Technologies in the Writing Process

The authors used ChatGPT only to improve the language of the Introduction and Discussion section, with an emphasis on improving clarity and correcting grammar. The scientific content was written entirely independently by the authors, without the use of AI tools. We hope that this clarification will resolve any issues with the use of AI in our submitted manuscript. The authors read the full article after using the AI tool and is responsible for the article.

Supplementary Material

Supplementary material associated with this article can be found, in the online version, at https://doi.org/10.31083/FBL26614.

References

[1] Murphy SJ, Werring DJ. Stroke: causes and clinical features. Medicine (Abingdon, England: UK Ed.). 2020; 48: 561–566. https://doi.org/10.1016/j.mpmed.2020.06.002.

[2] Alkahtani R. Molecular mechanisms underlying some major common risk factors of stroke. Heliyon. 2022; 8: e10218. https://doi.org/10.1016/j.heliyon.2022.e10218.

[3] Feigin VL, Brainin M, Norrving B, Martins S, Sacco RL, Hacke W, *et al*. World Stroke Organization (WSO): Global Stroke Fact Sheet 2022. International Journal of Stroke: Official Journal of the International Stroke Society. 2022; 17: 18–29. https://doi.org/10.1177/17474930211065917.

[4] Chen L, Xiao LD, Chamberlain D. An integrative review: Challenges and opportunities for stroke survivors and caregivers in hospital to home transition care. Journal of Advanced Nursing. 2020; 76: 2253–2265. https://doi.org/10.1111/jan.14446.

[5] Bindal P, Kumar V, Kapil L, Singh C, Singh A. Therapeutic management of ischemic stroke. Naunyn-Schmiedeberg's Archives of Pharmacology. 2024; 397: 2651–2679. https://doi.org/10.1007/s00210-023-02804-y.

[6] Shui X, Chen J, Fu Z, Zhu H, Tao H, Li Z. Microglia in ischemic stroke: pathogenesis insights and therapeutic challenges. Journal of Inflammation Research. 2024; 3335–3352. http://doi.org/10.2147/JIR.S461795.

[7] Lücht J, Rolfs N, Wowro SJ, Berger F, Schmitt KRL, Tong G. Cooling and Sterile Inflammation in an Oxygen-Glucose-Deprivation/Reperfusion Injury Model in BV-2 Microglia. Mediators of Inflammation. 2021; 2021: 8906561. https://doi.org/10.1155/2021/8906561.

[8] Li Y, Xu X, Wu X, Li J, Chen S, Chen D, *et al*. Cell polarization in ischemic stroke: molecular mechanisms and advances. Neural Regeneration Research. 2025; 20: 632–645. http://doi.org/10.4103/NRR.NRR-D-23-01336.

[9] Wu H, Zheng J, Xu S, Fang Y, Wu Y, Zeng J, *et al*. Mer regulates microglial/macrophage M1/M2 polarization and alleviates neuroinflammation following traumatic brain injury. Journal of Neuroinflammation. 2021; 18: 2. https://doi.org/10.1186/s12974-020-02041-7.

[10] Grefkes C, Fink GR. Recovery from stroke: current concepts and future perspectives. Neurological Research and Practice. 2020; 2: 17. https://doi.org/10.1186/s42466-020-00060-6.

[11] Hamdan TA, Lang PA, Lang KS. The Diverse Functions of the Ubiquitous Fcγ Receptors and Their Unique Constituent, FcRγ Subunit. Pathogens (Basel, Switzerland). 2020; 9: 140. https://doi.org/10.3390/pathogens9020140.

[12] Weng W, Cheng F, Zhang J. Specific signature biomarkers

highlight the potential mechanisms of circulating neutrophils in aneurysmal subarachnoid hemorrhage. Frontiers in Pharmacology. 2022; 13: 1022564. https://doi.org/10.3389/fphar.2022.1022564.

[13] Minett T, Classey J, Matthews FE, Fahrenhold M, Taga M, Brayne C, *et al*. Microglial immunophenotype in dementia with Alzheimer's pathology. Journal of Neuroinflammation. 2016; 13: 1–10. https://doi.org/10.1186/s12974-016-0601-z.

[14] Bao H, Li J, Zhang B, Huang J, Su D, Liu L. Integrated bioinformatics and machine-learning screening for immune-related genes in diagnosing non-alcoholic fatty liver disease with ischemic stroke and RRS1 pan-cancer analysis. Frontiers in Immunology. 2023; 14: 1113634. https://doi.org/10.3389/fimmu.2023.1113634.

[15] Xu X, Gao W, Li L, Hao J, Yang B, Wang T, *et al*. Annexin A1 protects against cerebral ischemia-reperfusion injury by modulating microglia/macrophage polarization via FPR2/ALX-dependent AMPK-mTOR pathway. Journal of Neuroinflammation. 2021; 18: 119. https://doi.org/10.1186/s12974-021-02174-3.

[16] Sun Z, Gu L, Wu K, Wang K, Ru J, Yang S, *et al*. VX-765 enhances autophagy of human umbilical cord mesenchymal stem cells against stroke-induced apoptosis and inflammatory responses via AMPK/mTOR signaling pathway. CNS Neuroscience & Therapeutics. 2020; 26: 952–961. https://doi.org/10.1111/cns.13400.

[17] Puthdee N, Sriswasdi S, Pisitkun T, Ratanasirintrawoot S, Israsena N, Tangkijvanich P. The LIN28B/TGF-β/TGFBI feedback loop promotes cell migration and tumour initiation potential in cholangiocarcinoma. Cancer Gene Therapy. 2022; 29: 445–455. https://doi.org/10.1038/s41417-021-00387-5.

[18] Saini V, Guada L, Yavagal DR. Global Epidemiology of Stroke and Access to Acute Ischemic Stroke Interventions. Neurology. 2021; 97: S6–S16. https://doi.org/10.1212/WNL.0000000000012781.

[19] Zhao XY, Hu SY, Yang JL, Chen XM, Huang XL, Tang LJ, *et al*. A 3' Untranslated Region Polymorphism of CTNNB1 (Rs2953) Alters MiR-3161 Binding and Affects the Risk of Ischemic Stroke and Coronary Artery Disease in Chinese Han Population. European Neurology. 2021; 84: 85–95. https://doi.org/10.1159/000514543.

[20] Xu X, Bass B, McKillop WM, Mailloux J, Liu T, Geremia NM, *et al*. Sox9 knockout mice have improved recovery following stroke. Experimental Neurology. 2018; 303: 59–71. https://doi.org/10.1016/j.expneurol.2018.02.001.

[21] Zielińska-Turek J, Dorobek M, Turek G, Dąbrowski J, Ziemba A, Andziak P, *et al*. MMP-9, TIMP-1 and S100B protein as markers of ischemic stroke in patients after carotid artery endarterectomy. Polski Merkuriusz Lekarski: Organ Polskiego Towarzystwa Lekarskiego. 2022; 50: 177–182.

[22] Babu M, Singh N, Datta A. In Vitro Oxygen Glucose Deprivation Model of Ischemic Stroke: A Proteomics-Driven Systems Biological Perspective. Molecular Neurobiology. 2022; 59: 2363–2377. https://doi.org/10.1007/s12035-022-02745-2.

[23] Băcilă CI, Vlădoiu MG, Văleanu M, Moga DFC, Pumnea PM. The Role of IL-6 and TNF-Alpha Biomarkers in Predicting Disability Outcomes in Acute Ischemic Stroke Patients. Life. 2025; 15: 47. https://doi.org/10.3390/life15010047.

[24] Wu CC, Chang CY, Shih KC, Hung CJ, Wang YY, Lin SY, *et al*. β-Funaltrexamine Displayed Anti-inflammatory and Neuroprotective Effects in Cells and Rat Model of Stroke. International Journal of Molecular Sciences. 2020; 21: 3866. https://doi.org/10.3390/ijms21113866.

[25] Yang C, Gong S, Chen X, Wang M, Zhang L, Zhang L, *et al*. Analgecine regulates microglia polarization in ischemic stroke by inhibiting NF-κB through the TLR4 MyD88 pathway. International Immunopharmacology. 2021; 99: 107930. https://doi.org/10.1016/j.intimp.2021.107930.

[26] Zhang W, Tian T, Gong SX, Huang WQ, Zhou QY, Wang AP, *et al*. Microglia-associated neuroinflammation is a potential therapeutic target for ischemic stroke. Neural Regeneration Research. 2021; 16: 6–11. https://doi.org/10.4103/1673-5374.286954.

[27] Zou J, Huang GF, Xia Q, Li X, Shi J, Sun N. Electroacupuncture promotes microglial M2 polarization in ischemic stroke via annexin A1. Acupuncture in Medicine: Journal of the British Medical Acupuncture Society. 2022; 40: 258–267. https://doi.org/10.1177/09645284211057570.

[28] Zhou X, Zhang YN, Li FF, Zhang Z, Cui LY, He HY, *et al*. Neuronal chemokine-like-factor 1 (CKLF1) up-regulation promotes M1 polarization of microglia in rat brain after stroke. Acta Pharmacologica Sinica. 2022; 43: 1217–1230. https://doi.org/10.1038/s41401-021-00746-w.

[29] Lei W, Zhuang H, Huang W, Sun J. Neuroinflammation and energy metabolism: a dual perspective on ischemic stroke. Journal of Translational Medicine. 2025; 23: 413. https://doi.org/10.1186/s12967-025-06440-3.

[30] Ahmadzadeh AM, Pourbagher-Shahri AM, Forouzanfar F. Neuroprotective effects of phytochemicals through autophagy modulation in ischemic stroke. Inflammopharmacology. 2025; 33: 1–29. http://doi.org/10.1007/s10787-024-01606-9.

[31] Zhao M, Dong Y, Chen L, Shen H. Influencing factors of stroke in patients with type 2 diabetes: A systematic review and meta-analysis. PloS One. 2024; 19: e0305954. https://doi.org/10.1371/journal.pone.0305954.

[32] Yuan Y, Xia F, Gao R, Chen Y, Zhang Y, Cheng Z, *et al*. Kaempferol Mediated AMPK/mTOR Signal Pathway Has a Protective Effect on Cerebral Ischemic-Reperfusion Injury in Rats by Inducing Autophagy. Neurochemical Research. 2022; 47: 2187–2197. https://doi.org/10.1007/s11064-022-03604-1.

[33] Wang L, Dai M, Ge Y, Chen J, Wang C, Yao C, *et al*. EGCG protects the mouse brain against cerebral ischemia/reperfusion injury by suppressing autophagy *via* the AKT/AMPK/mTOR phosphorylation pathway. Frontiers in Pharmacology. 2022; 13: 921394. https://doi.org/10.3389/fphar.2022.921394.